Saudi Pharmaceutical Journal 28 (2020) 1605–1615

Contents lists available at ScienceDirect

Saudi Pharmaceutical Journal

journal homepage: www.sciencedirect.com

Original article

Differential modulation of Ahr and Arid5a: A promising therapeutic strategy for autoimmune encephalomyelitis

Abdullah Alzahrani [a,1], Hamza Hanieh [a,b,*,1]

[a] Biological Sciences Department, King Faisal University, Al-Ahsa, Hofouf, Saudi Arabia
[b] Department of Medical Analysis, Department of Biological Sciences, Al Hussein bin Talal University, Ma'an, Jordan

ARTICLE INFO

Article history:
Received 9 August 2020
Accepted 18 October 2020
Available online 28 October 2020

Keywords:
Ahr
Arid5a
Inflammation
Autoimmunity
Multiple sclerosis
Therapeutic

ABSTRACT

Multiple sclerosis (MS) is an autoimmune disease that involves demyelination of axons in the central nervous system (CNS) and affects patients worldwide. It has been demonstrated that ligand-activated aryl hydrocarbon receptor (Ahr) ameliorates experimental autoimmune encephalomyelitis (EAE), a murine model of MS, by increasing $CD4^+FoxP3^+$ T cells. Recent evidence indicates that AT-rich interactive domain-containing protein 5a (Arid5a) is required for EAE pathogenesis by stabilizing *Il6* and *OX40* mRNAs. However, the differential modulation of Ahr and Arid5a in autoimmunity as a therapeutic strategy is unexplored. Herein, an *in silico*, *in vitro* and *in vivo* approach identified Flavipin (3,4,5-trihydroxy-6-methylphthalaldehyde) as an Ahr agonist that induces the expression of Ahr downstream genes in mouse $CD4^+$ T cells and $CD11b^+$ macrophages. Interestingly, Flavipin inhibited the stabilizing function of Arid5a and its counteracting effects on Regnase-1 on the 3′ untranslated region (3′UTR) of target mRNAs. Furthermore, it inhibited the stabilizing function of Arid5a on *Il23a* 3′UTR, a newly identified target mRNA. In EAE, Flavipin ameliorated disease severity, with reduced $CD4^+IL\text{-}17^+$ T cells, IL-6 and TNF-α and increased $CD4^+FoxP3^+$ T cells. Moreover, EAE amelioration was concomitant with reduced $CD4^+OX40^+$ and $CD4^+CD45^+$ T cells in the CNS. RNA interference showed that the modulatory effects of Flavipin on pro- and anti-inflammatory mediators in $CD4^+$ T cells and macrophages were Ahr- and/or Arid5a-dependent. In conclusion, our findings reveal differential modulation of Ahr and Arid5a as a new therapeutic strategy for MS.

1. Introduction

Multiple sclerosis (MS) is a neurodegenerative autoimmune disease characterized by demyelination in the central nervous system (CNS). It affects over 2.5 million people worldwide and is a major cause of different levels of disabilities among young adults (Van Schependom et al., 2019). A number of studies at the transcriptional regulatory level have provided valuable information about the mechanisms underlying MS pathogenesis, and this information has opened new opportunities for therapeutic strategies in MS (Srinivasan et al., 2017; Yan et al., 2018). Recently, RNA-binding proteins (RBPs) have emerged as new players in the development of MS owing to their ability to modify the transcriptome during inflammatory and autoimmune responses (Hanieh et al., 2018; Salapa et al., 2020). However, few studies have linked proteins from these two regulatory levels as a potential therapeutic strategy for MS.

Aryl hydrocarbon receptor (Ahr) is a ligand-activated transcription factor implicated in several aspects of autoimmune inflamma-

Abbreviations: MS, multiple sclerosis; CNS, central nervous system; Ahr, aryl hydrocarbon receptor; EAE, experimental autoimmune encephalomyelitis; Arid5a, AT-rich interactive domain-containing protein 5a; miR, microRNA; 3′UTR, 3′ untranslated region; RBP, RNA-binding protein; Arnt, Ahr nuclear translocator; RIP, RNA immunoprecipitation; LPS, lipopolysaccharide; ActinD, actinomycin D; PAS-A and PAS-B, Per-Arnt-Sim domain; SPF, specific pathogen-free; CFA, complete Freund's adjuvant; $MOG_{35\text{-}55}$, myelin oligodendrocyte glycoprotein.

* Corresponding author at: Department of Medical Analysis, Al Hussein bin Talal University, Ma'an 71111, P. Box 20, Jordan.
E-mail address: hhanieh@ahu.edu.jo (H. Hanieh).
[1] Co-first authors.

Peer review under responsibility of King Saud University.

Production and hosting by Elsevier

https://doi.org/10.1016/j.jsps.2020.10.007
1319-0164/

tion (Masuda et al., 2011; Nakahama et al., 2011; Chinen et al., 2015). It forms a complex with Ahr nuclear translocator (Arnt) in response to structurally diverse ligands to induce a battery of downstream genes that mediate its immunomodulatory properties (Nakahama et al., 2013; Nguyen et al., 2013; Hanieh, 2014). Several exogenous Ahr ligands have been examined for their anti-inflammatory potential in animal models of autoimmune diseases. For example, norisoboldine (Tong et al., 2016) and mesalamine (Oh-oka et al., 2017) alleviate autoimmune conditions by promoting the differentiation of regulatory T (Treg) cells and reducing pro-inflammatory mediators *via* the Ahr pathway in animal models of arthritis (Tong et al., 2016), and colitis (Oh-oka et al., 2017).

In experimental autoimmune encephalomyelitis (EAE), a well-established murine model of MS, activation of Ahr by laquinimod mitigates disease severity by enhancing differentiation of Treg cells and suppressing pro-inflammatory cytokines (Kaye et al., 2016). Tryptophan metabolites in combination with type I interferons limit CNS inflammation in EAE mice through activation of Ahr signaling in astrocytes (Rothhammer et al., 2016). Furthermore, activation of Ahr by 2,3,7,8-tetrachlorodibenzo-p-dioxin (TCDD) and gallic acid ameliorates EAE through microRNA (miR)-132-mediated cholinergic anti-inflammation and suppression of IL-6 and IL-17 (Hanieh and Alzahrani, 2013; Alzahrani et al., 2019), while gallic acid regulates the pathogenic potential of microglia and astrocytes (Alzahrani et al., 2019). Therefore, activation of Ahr may be a valuable therapeutic strategy to control autoimmune inflammation.

Recently, posttranscriptional regulation of inflammation and autoimmunity by RBPs has attracted research interest due to the ability of these factors to control the half-lives of related mRNAs. It has been demonstrated that dysfunction of heterogeneous nuclear ribonucleoprotein A1 (hnRNP A1) (Douglas et al., 2016), tristetraprolin (TTP) (Patial et al., 2016), and AU-rich element RNA-binding protein 1 (AUF1) (Sadri and Schneider, 2009) induces inflammation and systemic autoimmunity. Regnase-1 (*Zc3h12a*)-deficient mice exhibit several pathologies of autoimmune diseases (Yoshinaga and Takeuchi, 2019). It destabilizes *Il6* and *Nfkbiz* (IκBζ) mRNAs through their 3′ untranslated region (3′UTR) and inhibits IL-17 signaling; therefore, *Zc3h12a*$^{+/-}$ mice exhibit exacerbated pulmonary inflammation and EAE (Garg et al., 2015).

Conversely, AT-rich interactive domain-containing protein 5a (Arid5a) is required for inflammatory immune responses and autoimmunity (Masuda et al., 2016; Zaman et al., 2016; Nyati et al., 2019; Metwally et al., 2020). It promotes EAE severity by stabilizing *Il6* and *OX40* mRNAs (Masuda et al., 2013; Hanieh et al., 2018). Arid5a triggers IL-17 signaling and enhances the mRNA stability of *Il6*, chemokine (C-X-C motif) ligand 1 (*Cxcl1*) and *Cxcl5* by binding to their 3′UTR and counteracting the RNase activity of Regnase-1 (Amatya et al., 2018). Furthermore, Arid5a competes with Regnase-1 and/or Roquin-1 and mitigates their RNA destabilizing functions on conserved stem-loop structures in the 3′UTR of signal transducer and activator of transcription 3 (*Stat3*) and CD134 (*OX40*) mRNAs (Masuda et al., 2016; Hanieh et al., 2018). Therefore, blocking Arid5a may be a potential therapeutic strategy for inflammatory and autoimmune diseases (Masuda and Kishimoto, 2018).

In the current study, we combined computational prediction, *in vitro* and *in vivo* studies to manipulate the functions of Ahr and Arid5a differentially as a new therapeutic strategy for MS and identified example molecule, namely Flavipin (3,4,5-trihy droxy-6-methylphthalaldehyde), as a new Ahr agonist with inhibitory effects on Arid5a functions in mice. Furthermore, we demonstrated the anti-inflammatory properties of Flavipin in EAE, provided a mechanistic explanation, and identified *Il23a* as a new mRNA target for Arid5a.

2. Materials and methods

2.1. In silico computational prediction

The PAS-B 3D structure was predicted and validated as previously described (Hanieh et al., 2016). Briefly, the PAS-B 3D model was developed using PS2 software (http://www.ps2.life.nctu.edu.tw/), and validated for stereochemical quality using SAVES version v5.0 software (https://services.mbi.ucla.edu/SAVES/). The Arid5a 3D structure was predicted as described elsewhere (Masuda et al., 2016). Briefly, the model was constructed using Spanner (Lis et al., 2011) and HHPred (Söding et al., 2005) with the MRF-2 domain (PDB ID: 1ig6). The chemical structure of Flavipin (CID_3083587) was retrieved from the PubChem database (www.ncbi.nlm.nih.gov/pccompound). Potential interactions of Flavipin with Ahr and Arid5a were studied by docking simulation using Autodock v1.5.4 and Autodock v4.2 software (http://www.scripps.edu/mb/olson/doc/autodock).

2.2. Experimental animals

Female C57BL/6 mice (6–8 weeks) were purchased originally from Charles River Laboratories (CA, USA), and Rag-1$^{-/-}$ mice were from Jackson Laboratory (ME, USA). The mice were maintained in specific pathogen-free (SPF) environments and had *ad libitum* access to feed and water. The experiments were performed according to the approved protocols by the Standing Research Ethics Committee, King Faisal University, Saudi Arabia. A body weight loss of ≥25% and paresis or forelimb paralysis for 24 h were considered humane endpoints.

2.3. Cell isolation and stimulation

To isolate naïve (CD4$^+$CD62L$^+$) T cells, a MACS isolation kit (Miltenyi Biotec, Bergisch Gladbach, Germany) was used. The conditions for the differentiation of Th17 and Treg cells were adopted from previous report with modifications (Nakahama et al., 2011). Briefly, naïve CD4$^+$ T cells were cultured in the presence of Mouse T-Activator CD3/CD28 Dynabeads (Invitrogen, CA, USA). To generate Th17 cells, the cell culture was supplemented with IL-6 (25 ng/mL; R&D Systems, MN, USA), TGF-β1 (3 ng/mL; R&D Systems), and anti-IFN-γ and anti-IL-4 antibodies (10 μg/mL; BioLegend, CA, USA). To generate Treg cells, the cell culture was supplemented with TGF-β1 (4 ng/mL; R&D Systems) and IL-2 (25 U/mL; R&D Systems). The thioglycolate (TGC)-recruited peritoneal macrophages were cultured in the presence of LPS (Sigma-Aldrich, MO, USA) at a concentration of 0.5 μg/mL. Purified Flavipin (3,4,5-trihydroxy-6-methylphthalaldehyde; 95–98%) was purchased from Chemieliva Pharmaceutical (Chongqing, China) and dissolved in DMSO.

2.4. Quantitative PCR

cDNA was synthesized from total RNA using TaqMan Reverse Transcription kits (Applied Biosystems, CA, USA). cDNA amplification was performed using a real-time PCR system (ViiA7; Applied Biosystems) with standard cycling conditions of 50 °C for 2 min and 95 °C for 10 min, followed by 40 cycles of 95 °C for 15 s and 60 °C for 1 min. The TaqMan Gene Expression Assays (Applied Biosystems) used were *Cyp1A1*, Mm00487218_m1; *Stat3*, Mm01219775_m1; *Tnfrsf4* (*OX40*), Mm00442039_m1; *AChE*, Mm00477274_g1; *Il23a*, Mm00518984_m1; *Rorc*, Mm01261022_m1; *Foxp3*, Mm00475162_m1; *Il6*, Mm00446190_m1; *Gapdh*, Mm99999915_g1; *has-miR-132*, ID:00457; *has-miR-212*, ID:00515; *RNU6B*, ID:1093.

2.5. Protein quantification

For western blotting, the cell lysates were separated by SDS-PAGE. The proteins were detected using validated rabbit polyclonal anti-Cyp1A1 antibodies (Santa Cruz Biotechnology, CA, USA), anti-Ahr antibodies (Santa Cruz Biotechnology), anti-Arid5a antibodies (Abcam, MA, USA), and mouse monoclonal anti-β-actin antibodies (Cell Signaling, MA, USA). The intensities of the protein bands were quantified using ImageJ v.1.48 software (http://imagej.nih.gov/ij/download.html). ELISA kits were used to quantify IL-17 and TGF-β (Quantikine; R&D Systems) and IL-6, TNF-α and IL-23a (Invitrogen), following the manufacturer's guidelines.

2.6. Plasmids

The pGL3 plasmids encoding the 3′UTR of *OX40* or *Il23a* were constructed by cloning the inserts at the XbaI restriction site using the In-Fusion HD Cloning Kit (Clontech, CA, USA). The primers used to synthesize the inserts were *OX40* (1076–1119) F: 5′-AGATCGC CGTGTAATTCTAGATCCTGATGCCTGCCAGTACCC-3′, R: 5′-GCCGGCC GCCCCGACTCTAGAAAGCCCAGAGCCAGCCCAGCACC-3′; *Il23a* (complete), F: 5′-AGATCGCCGTGTAATTCTAGAAGACCCAGAGAGCCACA TAA-3′, R: 5′-GCCGGCCGCCCCGACTCTAGATGAGCCCTTAGTGCCAA CAG-3′. Mouse protein expression plasmids (Arid5a, Regnase-1; pcDNA3.1) cloned at the EcoR1 and XbaI restriction sites and pGL3 plasmids encoding the 3′UTR of *Il6* and *Stat3* cloned at the XbaI restriction site were generously provided by Professor Tadamitsu Kishimoto, Osaka University, Japan.

2.7. Transfection and luciferase activity

HEK293T cells (ATCC, ME, USA) were transfected with the plasmids using Lipofectamine LTX (Invitrogen) for 48 h. The luciferase activities (Firefly) normalized to *Renilla* were quantified using the Dual-Luciferase Reporter System (Promega, WI, USA) following the manufacturer's guidelines. $CD4^+CD62L^+$ T cells and peritoneal macrophages were electroporated with Ahr siRNA (siAhr; 100 nM; Ambion, MA, USA), siArid5a (100 nM; Sigma-Aldrich), or nonspecific (siNS; 100 nM; Ambion) by a 4D-Nucleofector System using specific transfection kits (Lonza, Cologne, Germany).

2.8. EAE models and treatment

EAE was induced following a modified method described previously (Nakahama et al., 2013). Briefly, MOG_{35-55} (125 μg/mL; Peptides International, KY, USA) emulsified in complete Freund's adjuvant (CFA; Sigma-Aldrich) containing H37RA (*Mycobacterium tuberculosis*; Difco Laboratories, NJ, USA) was injected at the base of the tail. On days 0 and 2, the mice received intraperitoneal injections of pertussis toxin (300 ng; Sigma-Aldrich). The scoring system was adopted as described elsewhere (Hanieh and Alzahrani, 2013) and assessed by expert who is blinded of experimental details; 0, normal; 1, limp tail; 2, hind limb paresis; 3, forelimb weakness; 4, paralysis; and 5, moribund. For adoptive transfer, $CD4^+$ T cells isolated from EAE mice 10 days post immunization were cultured for 72 h with MOG_{35-55} (25 μg/mL) and IL-23 (25 ng/mL). The encephalitogenic cells (1×10^7 cell/mouse) were injected intravenously into Rag-$1^{-/-}$ mice. For Flavipin treatment, the mice received intraperitoneal injections with vehicle (corn oil) or Flavipin (1.5 mg/mouse/day) for 11 consecutive days starting one day prior to MOG_{35-55} immunization and ending before onset of clinical symptoms.

2.9. RIP and mRNA stability assays

Peritoneal macrophages were stimulated with LPS for 3 h. The RNA immunoprecipitation (RIP) assay kit (MBL International, MA, USA) and anti-Arid5a antibodies (Abcam) were used to detect *Il23a* mRNA in the lysates. For mRNA stability, LPS-stimulated macrophages (3 h) were treated with actinomycin D (ActinD; 5 μg/mL) for 0–3 h. The RNA isolated from RIP and stability assays was analyzed using quantitative real-time PCR.

2.10. Flow cytometry

The $CD4^+$ T cells were stimulated with ionomycin (800 ng/mL; Sigma-Aldrich) and phorbol 12-myristate 13-acetate (50 ng/mL; Sigma-Aldrich) for 5 h, and Protein Transport Inhibitor (Invitrogen) was added for the last 2 h. Phycoerythrin (PE)-conjugated anti-IL-17 antibodies (eBioscience, CA, USA) and an intracellular staining kit (Life Technologies) were used. Fluorescein isothiocyanate (FITC)-conjugated anti-Foxp3 antibodies and a Foxp3 staining kit (Invitrogen) were used following the manufacturer's guidelines. PerCP-Cy5.5-conjugated anti-CD4 antibodies (eBioscience), and PE-conjugated anti-OX40 (BioLegend) antibodies were used for surface staining. The analysis was carried out using a FlowSight system (Amnis, TX, USA).

2.11. Statistics

Three independent experiments were carried out in triplicate, unless otherwise indicated. Data are shown as the mean ± SD of representative experiments. The differences between means were analyzed by one-way ANOVA. The statistical significance of the EAE clinical score and RNA stability results was analyzed by two-way ANOVA. The statistical significance of EAE incidence was analyzed by X^2 test. $^*p < 0.05$ was considered significant.

3. Results

3.1. In silico potential for interaction of Flavipin with Ahr and Arid5a

We previously found that activation of Ahr by exogenous ligands and deletion of Arid5a ameliorates EAE in mice (Hanieh and Alzahrani, 2013; Hanieh et al., 2018; Alzahrani et al., 2019). Therefore, we hypothesized that differential modulation of Ahr and Arid5a using an exogenous molecule would be a new therapeutic strategy for MS; therefore, we first carried out a molecular docking screening using a customized hydrocarbon library.

Among the tested molecules, Flavipin showed potential interactions with both Ahr and Arid5a. Analysis of the computational simulation revealed that Flavipin forms five hydrogen bonds with the Arg7 and Cys19 residues of the ligand-binding domain of mouse Ahr, namely, PAS-B, with a binding energy of −3.48 kcal/mol (Fig. 1A). In addition, a van der Waals force was predicted to occur with residue Lys58. Docking simulation of Flavipin was carried out against the ARID domain (Glu50 to Leu146) of mouse Arid5a (Masuda et al., 2016). The analysis showed that Flavipin forms three hydrogen bonds with residues Arg127, Glu131 and Arg132 with a binding energy of −3.05 kcal/mol (Fig. 1B). Furthermore, van der Waals forces were predicted with the residues Glu131 and Leu135. Collectively, these observations suggest Flavipin as a candidate molecule with dual interactions with Ahr and Arid5a.

3.2. Ahr downstream genes are induced by Flavipin

Having identified Flavipin as a potential ligand for Ahr, we first tested whether Flavipin induces the expression of Ahr downstream genes in cells implicated in EAE pathogenesis. Therefore, the gene expression of cytochrome P450 1A1 (*Cyp1A1*) was quantified in $CD4^+$ T cells cultured in Th17 cell-inducing conditions and in macrophages cultured in the presence of lipopolysaccharide (LPS). As depicted in Fig. 2A and B, Flavipin (20–80 μM) upregulated the

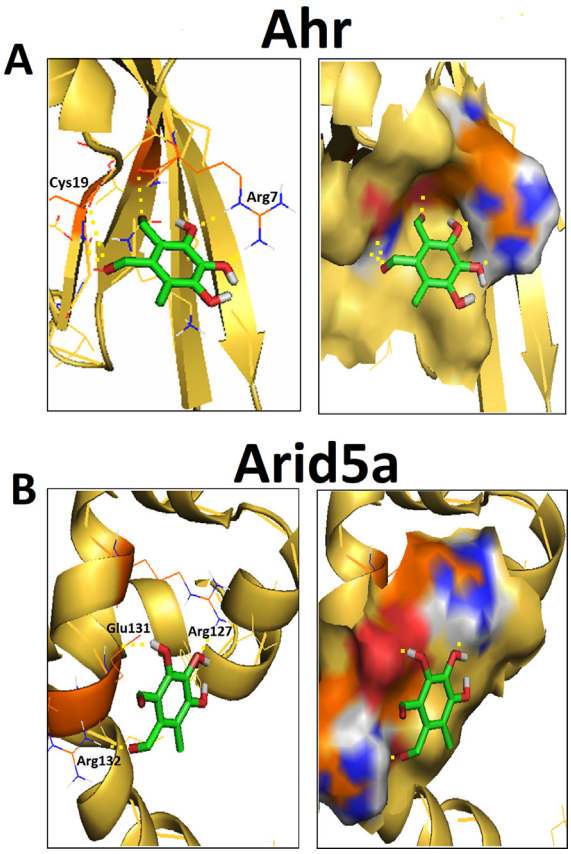

Fig. 1. *In silico* binding potential of Flavipin to mouse Ahr and Arid5a. (A) Putative binding mode of Flavipin to the Ahr PAS-B domain; five hydrogen bonds were formed at Arg7 and Cys19. (B) Putative binding mode of Flavipin with the ARID domain (residues 50–146) of the Arid5a protein; three hydrogen bonds were formed at Arg127, Glu131 and Arg132. The yellow dotted lines indicate the hydrogen bonds. The right panels in A and B represents contour maps of the binding sites.

mRNA and protein expression of Cyp1A1 in both $CD4^+$ T cells cultured in Th17 cell conditions and LPS-stimulated macrophages in a concentration-dependent manner. The efficiency of cell stimulation *in vitro* is shown in Fig. S1. Treating cells with 120 μM Flavipin reduced cell viability (Fig. S2); therefore, a safe concentration of 40 μM was used for further investigation. Silencing Ahr abolished the Flavipin promoting effects on the expression of the *Cyp1A1* gene (Fig. 2C and D), indicating an Ahr-dependent mode of action.

We previously identified the miR-212/132 cluster as a new downstream gene of Ahr (Nakahama et al., 2013; Hanieh and Alzahrani, 2013; Hanieh, 2015). Therefore, the effects of Flavipin on the expression of miR-132 and miR-212 were assessed. As expected, Flavipin upregulated the expression of the miRNA cluster in differentiating Th17 cells and LPS-stimulated macrophages, but depletion of Ahr abrogated these enhancing effects (Fig. 2E). The efficiency of silencing Ahr using siAhr was confirmed (Fig. 2F). Collectively, these results suggest Flavipin as a new Ahr ligand in mice with agonistic properties.

3.3. Stabilizing functions and counteracting activity of Arid5a on Regnase-1 on the 3′UTR are abolished by Flavipin

Arid5a is required for autoimmunity *via* stabilizing the mRNAs of *Il6*, *Stat3* and *OX40* through their 3′UTRs (Masuda et al., 2013; Masuda et al., 2016; Hanieh et al., 2018). Therefore, we examined the stabilizing functions of Arid5a on the 3′UTRs of target mRNAs in the presence of Flavipin using HEK293T cells. Overexpression of Arid5a increased the luciferase activity of the pGL3 plasmid driven by the 3′UTR of *Il6*, *Stat3* or *OX40* (Fig. 3A). These enhancing effects of Arid5a on the luciferase activities were abolished with Flavipin at 40 μM (Fig. 3A). Afterward, we assessed the effects of Flavipin on the counteracting activity of Arid5a on the ribonuclease Regnase-1 on the 3′UTR of target mRNAs. Overexpression of Arid5a counteracted Regnase-1 suppressive effects on the luciferase activity of the pGL3 plasmid encoding the 3′UTR of *Il6*, *Stat3* or *OX40* (Fig. 3B). These counteracting effects of Arid5a were abrogated in the presence of Flavipin (Fig. 3B). Collectively, these findings indicate that Flavipin is an inhibitor of Arid5a function.

3.4. Ahr and Arid5a mediate the alleviative effects of Flavipin on EAE

To determine the biological significance of the differential actions of Flavipin on Ahr and Arid5a, we first examined its effects on EAE severity. Higher dose of Flavipin (6 mg/day/mouse) increased spleen and liver weights (Fig. S2). An optimized Flavipin treatment (1.5 mg/day/mouse) alleviated clinical and maximum scores of EAE compared to vehicle-treated (Control) mice (Fig. 4A) but not EAE incidence (Fig. 4B). These alleviating effects were concomitant with lower serum levels of IL-6 and TNF-α on day 23 post MOG_{35-55} immunization (Fig. 4C). Furthermore, $CD4^+$ T cells isolated from the inguinal lymph nodes of Flavipin-treated EAE mice on day 10 post immunization produced less IL-17 and more TGF-β in response to MOG_{35-55} restimulation (Fig. 4D). Consistent with these observations, the frequency of $CD4^+IL\text{-}17^+$ T cells was decreased and that of $CD4^+FoxP3^+$ T cells was increased in Flavipin-treated EAE mice (Fig. 4E).

Attenuation of EAE in $Arid5a^{-/-}$ mice is associated with a reduced frequency of $CD4^+OX40^+$ T cells and less infiltration of $CD4^+CD45^+$ T cells within the CNS (Hanieh et al., 2018). Comparably, the frequency of $CD4^+OX40^+$ T cells and infiltration of $CD4^+$-$CD45^+$ T cells within the CNS were reduced with Flavipin treatment (Fig. 4E and F). It has been previously shown that agonistic anti-OX40 antibodies (OX86) induce weak IL-17 production by encephalitogenic $Arid5a^{-/-}$ $CD4^+$ T cells compared to wild-type cells (Hanieh et al., 2018). Herein, we found that encephalitogenic $CD4^+$ T cells from Flavipin-treated EAE mice produced less IL-17 in response to MOG_{35-55} restimulation and ligation of OX40 with OX86 antibodies (Fig. 4G).

The effect of Flavipin on transcriptional activation of Ahr *in vivo* was examined by quantifying the mRNAs of downstream genes. As presented in Fig. 4H and I, the mRNA expression levels of *Cyp1A1*, miR-132 and miR-212 were upregulated in $CD4^+$ T cells isolated from spleens of Flavipin-treated mice with EAE on day 10 post MOG_{35-55} immunization. In $CD11b^+$ macrophages, the expression of *Cyp1A1* and miR-132 mRNAs was upregulated, whereas that of miR-212 did not reach a significance level (Fig. 4H and I). We previously showed that ligand-activated Ahr potentiates cholinergic anti-inflammation in animal models of autoimmune diseases by inducing the expression of acetylcholinesterase (AChE)-targeting miR-132 (Hanieh and Alzahrani, 2013; Alzahrani et al., 2017). As depicted in Fig. 4J, the mRNA expression of *AChE* was downregulated in splenocytes from Flavipin-treated EAE mice, indicating that Flavipin induced the miR-132/AChE module. Taken together, these findings indicate that Flavipin ameliorates EAE severity by activating Ahr and inducing its anti-inflammatory effects and by inhibiting Arid5a and blocking its pro-inflammatory functions.

3.5. Ahr-dependent and Arid5a-dependent mechanisms mediate the modulatory effects of Flavipin on cytokines

For further mechanistic illustration, we assessed the effects of Flavipin on the effector functions of $CD4^+$ T cells cultured in Th17- or Treg cell-inducing milieus and macrophages stimulated with LPS. Consistent with the *in vivo* results, Flavipin (40 μM)

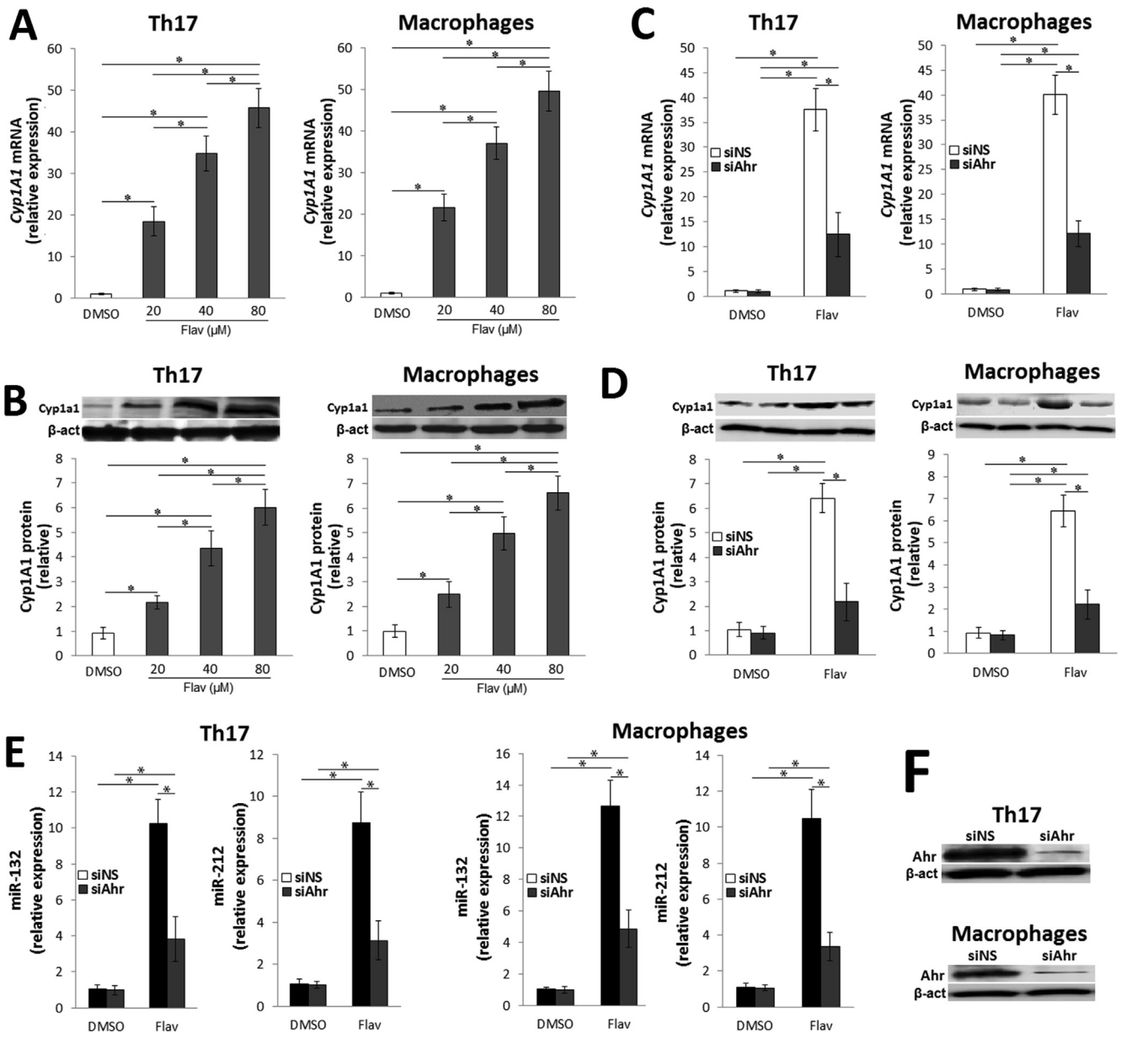

Fig. 2. The Ahr downstream genes are induced by Flavipin in an Ahr-dependent manner. Naïve T cells ($CD4^+CD62L^+$) were cultured under Th17-inducing conditions, and macrophages were stimulated with LPS. The expression of *Cyp1A1* and miR-212/132 cluster mRNAs was measured by real-time PCR and normalized to *Gapdh* or *RNU6B* mRNAs, respectively. Cyp1A1 protein was detected by immunoblot; actin was used as a loading control. (A) Relative mRNA expression of *Cyp1A1* in differentiating Th17 cells and macrophages (12 h) in the presence of Flavipin (Flav; 20–80 μM) compared to DMSO-treated cells. (B) Immunoblot and protein expression of Cyp1A1 in differentiating Th17 cells and macrophages (48 h) in the presence of Flavipin (20–80 μM) compared to DMSO treatment. (C) Relative expression of *Cyp1A1* mRNA in differentiating Th17 cells and macrophages (12 h) electroporated with nonspecific siRNA (siNS; 100 nM) or Ahr siRNA (siAhr; 100 nM) in the presence of Flavipin (40 μM) compared to DMSO treatment. (D) Immunoblot and relative protein expression of Cyp1A1 in differentiating Th17 cells and macrophages (48 h) electroporated with siAhr or siNS in the presence of Flavipin (40 μM) compared to DMSO treatment. (E) Relative expression of miR-132 and miR-212 in differentiating Th17 cells and macrophages (30 h) electroporated with siAhr or siNS in the presence of Flavipin (40 μM) compared to DMSO treatment. (F) The efficiency of siAhr was confirmed by immunoblot. Data are shown as the mean ± SD from representative experiment out of three independent experiments ($n = 3$ each) studied in triplicates and produced similar results. $^*p < 0.05$ (one-way ANOVA); horizontal bars denote statistical comparisons.

reduced the production of IL-17, IL-6, TNF-α and IL-23 and increased TGF-β production (Fig. 5A and B). Depletion of Ahr by siAhr in differentiating Th17 and Treg cells mitigated the suppressive effects of Flavipin on IL-17 production and cancelled its enhancing effects on TGF-β production compared with the nonspecific siRNA (siNS) counterpart (Fig. 5C). In LPS-stimulated macrophages, silencing Ahr by siAhr mitigated the suppressive effects of Flavipin on IL-6 and cancelled its effects on TNF-α but did not alter its effect on IL-23 compared with its siNS counterpart (Fig. 5D).

Subsequently, we depleted Arid5a by siArid5a. Silencing Arid5a in differentiating Th17 and Treg cells augmented the inhibitory effects of Flavipin on IL-17, but no effects were reported on TGF-β compared with the siNS counterpart (Fig. 5E). In LPS-stimulated macrophages, siArid5a augmented the inhibitory effects of Flavipin on IL-6 and IL-23 but did not

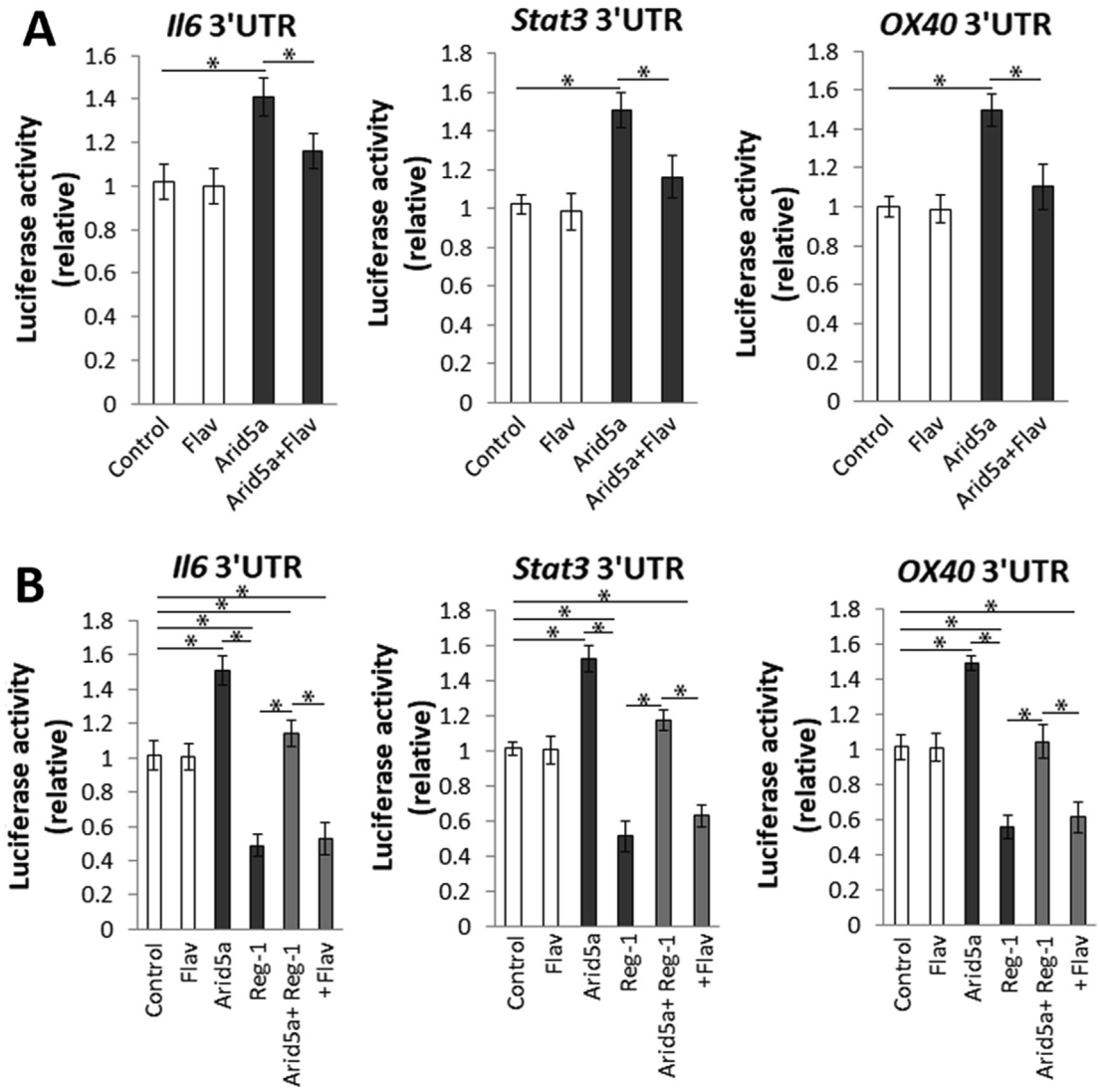

Fig. 3. Arid5a stabilizing functions and competition with Regnase-1 on the 3′UTR of target mRNAs are abolished by Flavipin. (A) Relative luciferase activity of pGL3 plasmids (100 ng) encoding the 3′UTR of *Il6*, *Stat3* or *OX40* (1076-1119) transfected into HEK293T cells (48 h) together with Arid5a expression plasmid (300 ng) compared with each activity when transfected with empty plasmid (Control; 300 ng); Flavipin (40 μM). (B) Relative luciferase activity of pGL3 plasmids (100 ng) encoding the 3′UTR of *Il6*, *Stat3* and *OX40* (1076-1119) transfected into HEK293T cells (48 h) together with Arid5a (300 ng) and/or Regnase-1 (300 ng) expression plasmids compared with each activity when transfected with empty plasmid (Control; 300–600 ng); Flavipin (40 μM). Data are shown as the mean ± SD from representative experiment out of three independent experiments studied in triplicates and produced similar results. $^{*}p < 0.05$ (one-way ANOVA); horizontal bars denote statistical comparisons.

exert significant effects on TNF-α compared to its siNS counterpart (Fig. 5F).

Arid5a stabilizes the mRNAs of *Stat3* and *OX40* during the differentiation of Th17 cells *in vitro* (Masuda et al., 2016; Hanieh et al., 2018). Therefore, we examined whether Flavipin affects the mRNA expression of these factors under similar conditions. As depicted in Fig. 5G, Flavipin downregulated the expression of *Stat3* and *OX40* mRNAs. Depletion of Arid5a abolished the suppressive effects of Flavipin on *Stat3* and *OX40* mRNAs compared with DMSO counterpart, whereas depletion of Ahr did not exert significant effects (Fig. 5G). The efficiency of siArid5a was confirmed (Fig. 5H) Taken together, the results suggest that Flavipin exerts its modulatory effects through Ahr-dependent and Arid5a-dependent mechanisms.

Finally, to examine whether the attenuating effects of Flavipin on EAE were mediated by T cells, EAE was induced by adoptive transfer of encephalitogenic $CD4^{+}$ T cells into Rag-1$^{-/-}$ mice. The clinical and maximum scores revealed that the $CD4^{+}$ T cells isolated from Flavipin-treated EAE mice induced mild symptoms (Fig. 5I). These observations indicate that Flavipin ameliorates EAE through T cell-dependent and T cell-independent mechanisms.

3.6. Il23a mRNA is a new target for Arid5a

We found that depletion of Arid5a by RNA interference results in comparable modulatory patterns of IL-6 and IL-23 in LPS-stimulated macrophages. Considering that *Il6* mRNA is an identified target for Arid5a (Masuda et al., 2013), we predicted that *Il23a* mRNA would be a target for Arid5a. Thus, we first studied whether Arid5a affects the luciferase activity of a pGL3 plasmid encoding the *Il23a* 3′UTR using HEK293T cells. Overexpression of Arid5a increased the luciferase activity of the pGL3 plasmid driven by the *Il23a* 3′UTR, and Flavipin treatment (40 μM) abolished the Arid5a-enhancing effects (Fig. 6A). Because physical binding of Arid5a to target mRNAs is required for its stabilizing function, we examined the association of Arid5a with *Il23a* mRNA by RIP assay. As shown in the real-time PCR amplification plot (Fig. 6B), *Il23a* mRNA was detected in the RNA eluate pulled down using

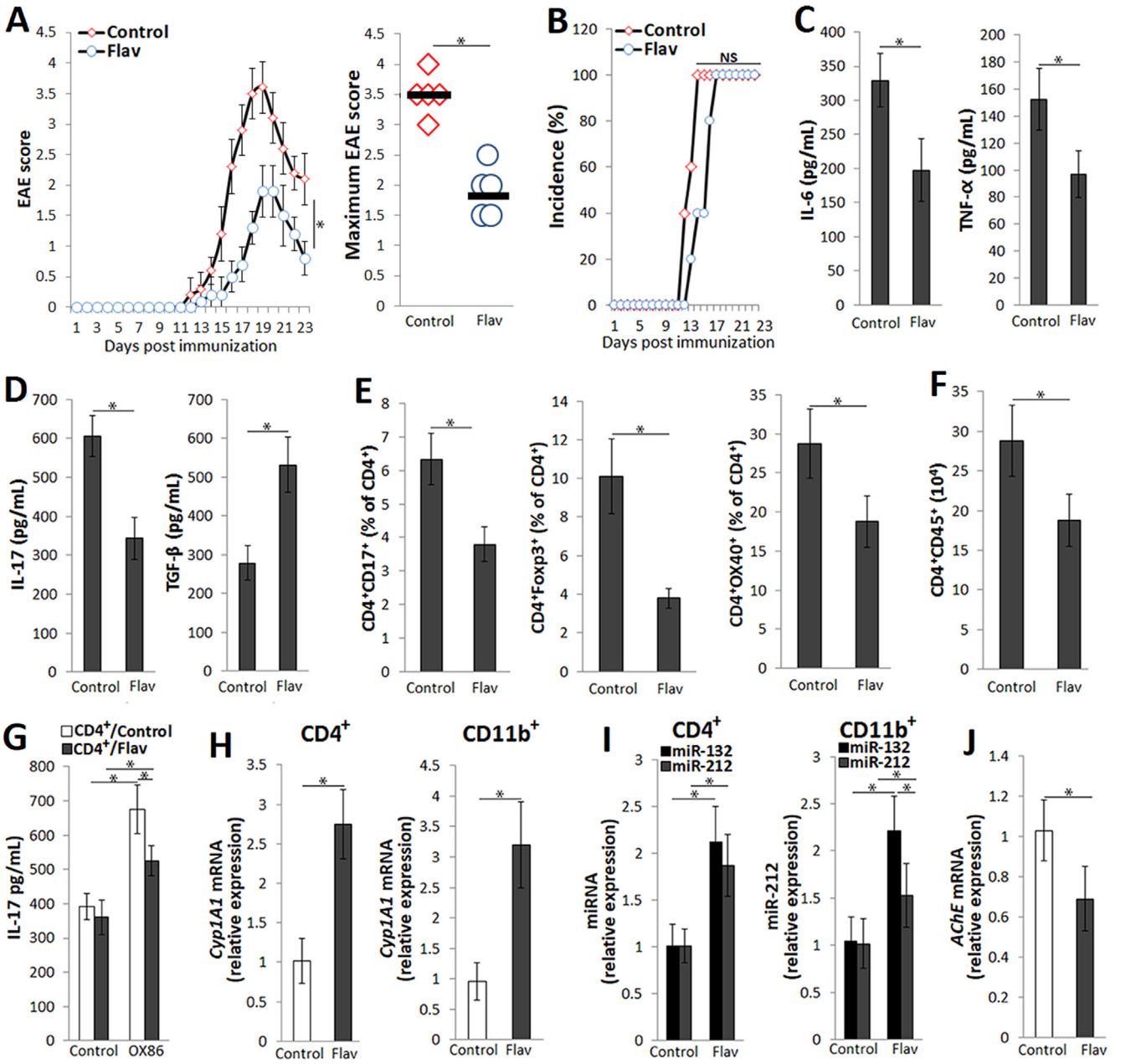

Fig. 4. Ahr- and Arid5a-dependent actions mediate the alleviating effects of Flavipin on EAE. MOG_{35-55} emulsified in CFA and pertussis toxin were used to induce EAE. The cytokines were quantified by ELISA, and the expression of mRNA encoding protein and miRNAs was assessed by real-time PCR and normalized to *Gapdh* or *RNU6B* mRNAs, respectively. (A) EAE clinical and maximum score and (B) incidence (%) in vehicle (Control)- or Flavipin (Flav)-treated mice. (C) Levels of IL-6 and TNF-α in the serum (day 23 post immunization). (D) Levels of IL-17 and TGF-β produced by encephalitogenic $CD4^+$ T cells isolated from the inguinal lymph nodes (10 days post immunization) and restimulated with MOG_{35-55} (72 h). (E) Flow cytometry analysis of the frequency (%) of $CD4^+IL\text{-}17^+$ and $CD4^+FoxP3^+$ T cells in the inguinal lymph nodes (day 23 post immunization) and the frequency of $CD4^+OX40^+$ T cells in the CNS (10 days post immunization), gated on $CD4^+$ T cells. (F) Absolute number of $CD4^+CD45^+$ T cells in the CNS (day 10 post immunization). (G) Culture supernatant level of IL-17 produced by encephalitogenic $CD4^+$ T cells restimulated as described in D in the absence (Control) or presence of agonistic anti-OX40 antibodies (OX86). (H) Relative expression of *Cyp1A1* mRNA in $CD4^+$ T cells and $CD11b^+$ macrophages isolated from the spleens of EAE mice (day 10 post immunization) compared to the control EAE mice. (I) Relative expression of miR-132 and miR-212 in $CD4^+$ T cells and $CD11b^+$ macrophages isolated from the spleens of EAE mice (10 post immunization) compared to the control EAE mice. (J) Relative expression of *AChE* mRNA in splenocytes from EAE mice (day 10 post immunization) compared to control EAE mice. Data in A and C-J are shown as the mean ± SD from representative experiment out of three independent experiments ($n = 5$ each) produced similar results; C-J were studied in triplicates. *$p < 0.05$, A left panel (two-way ANOVA); B (X^2 test); A right panel and C–J (one-way ANOVA); horizontal and vertical bars denote statistical comparisons.

Arid5a antibodies. Finally, the mRNA stability results confirmed that silencing Arid5a reduced the half-life of *Il23a* mRNA in LPS-stimulated macrophages after ActinD treatment. Collectively, these results suggest that Arid5a stabilizes the *Il23a* mRNA through an interaction with its 3′UTR.

4. Discussion

Accumulating evidence demonstrates that activation of Ahr by exogenous ligands alleviates EAE severity by boosting the differentiation of Treg cells and suppressing pro-inflammatory mediators

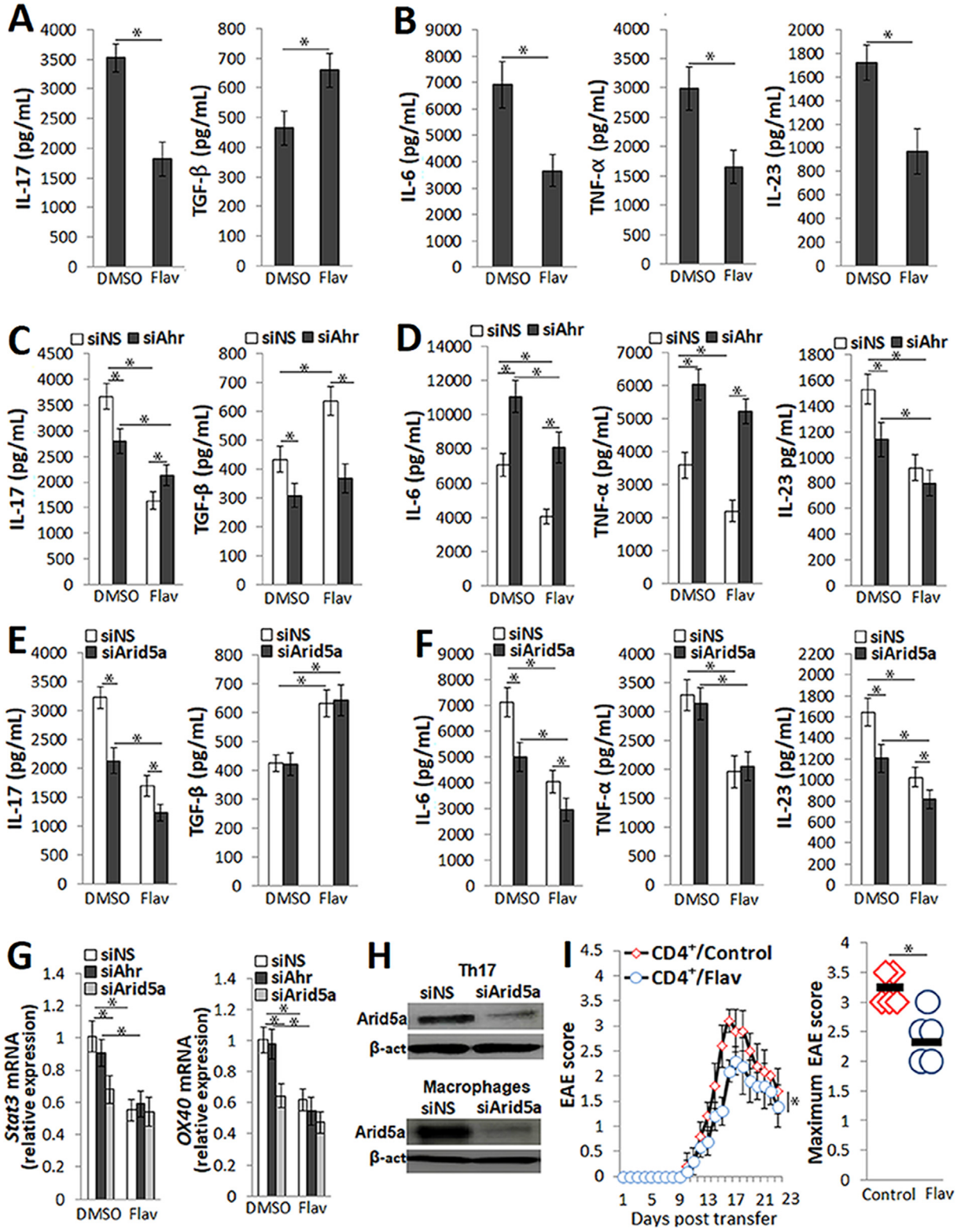

Fig. 5. The modulatory effects of Flavipin on cytokines are mediated by Ahr- and Arid5a-dependent effects. Naïve T cells ($CD4^+CD62L^+$) were cultured under Th17- or Treg-inducing conditions, and peritoneal macrophages were stimulated with LPS in presence or absence of Flavipin (40 μM). The cells were electroporated with nonspecific siRNA (siNS; 100 nM) or Ahr siRNA (siAhr; 100 nM), siArid5a or. Cytokines were measured using ELISA, and mRNAs were measured by real-time PCR and normalized to *Gapdh* mRNA. (A) Levels of IL-17 and TGF-β produced by $CD4^+$ T cells cultured under Th17- or Treg-inducing conditions (72 h), respectively. (B) Levels of IL-6, TNF-α and IL-23 produced by LPS-stimulated macrophages (16 h). (C and E) Levels of IL-17 and TGF-β produced by $CD4^+$ T cells electroporated with siAhr, siArid5a or siNS and cultured under Th17- or Treg-inducing conditions. (D and F) Levels of IL-6, TNF-α and IL-23 produced by macrophages electroporated with siAhr, siArid5a or siNS and stimulated with LPS. (G) Relative mRNA expression of *Stat3* and *OX40* in $CD4^+$ T cells cultured under Th17-inducing conditions (12 h) compared with DMSO-treated cells. (H) The efficiency of siArid5a was confirmed by immunoblot. (I) Clinical and maximum scores of EAE induced in Rag-$1^{-/-}$ mice by adoptive transfer of encephalitogenic $CD4^+$ T cells isolated from EAE mice (10 days post immunization) and restimulated with MOG_{35-55} (72 h). Data in A-G are shown as the mean ± SD of representative experiment out of three independent experiments (n = 3 each) studied in triplicates and produced similar results. Data in I (left panel) are shown as the mean ± SD from representative experiment out of two independent experiments (n = 5 each) produced similar results; I (right panel) represents individual animals. *p < 0.05, A-G and I right panel (one-way ANOVA); I left panel (two-way ANOVA); horizontal and vertical bars denote statistical comparisons.

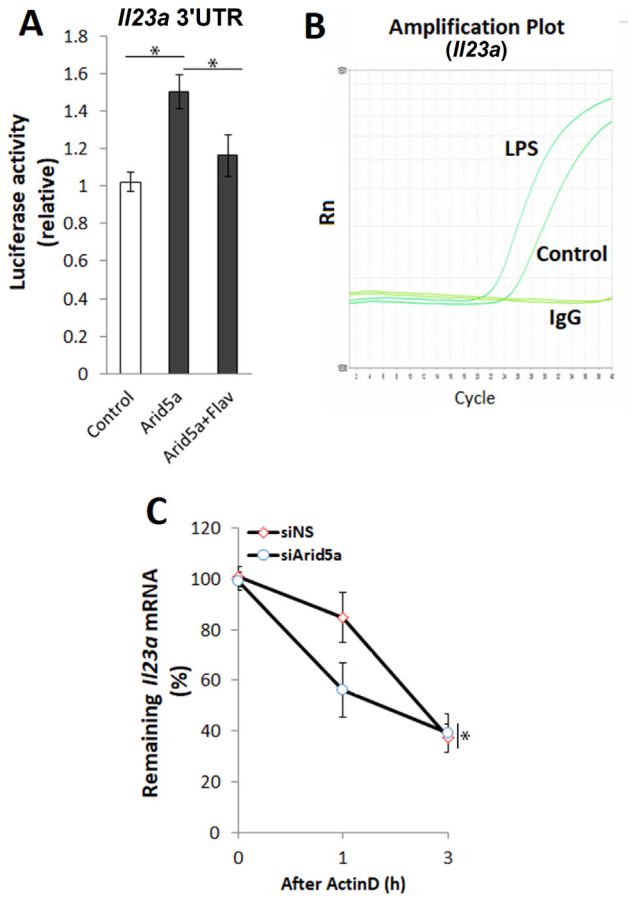

Fig. 6. *Il23a* is a new mRNA target for Arid5a. (A) Relative luciferase activity of a pGL3 plasmid encoding the 3′UTR of *Il23a* (100 ng) transfected into HEK293T cells (48 h) together with the Arid5a expression plasmid (300 ng) compared with its activity when transfected with the empty plasmid (Control; 300 ng); Flavipin (40 μM). (B) Representative real-time PCR amplification plot of *Il23a* in the RNA eluate obtained from LPS-stimulated macrophages (3 h) using anti-Arid5a and control IgG antibodies (RIP assay). (C) Relative expression of *Il23a* mRNA in LPS-stimulated macrophages for 3 h and then treated for 0–3 h with actinomycin D (ActinD) compared to mRNA expression at 0 h. (A and C) Data are shown as the mean ± SD from representative experiment out of three independent experiments studied in triplicates and produced similar results; C (n = 3 each). $^*p < 0.05$, A (one-way ANOVA); C (two-way ANOVA); horizontal bars denote statistical comparisons.

(Hanieh and Alzahrani, 2013; Kaye et al., 2016; Alzahrani et al., 2019). Recent evidence indicates that Arid5a is required for EAE pathogenesis by stabilizing mRNAs encoding related proteins (Masuda et al., 2013; Hanieh et al., 2018). However, there are no reports on studies involving manipulation of the functions of Ahr and Arid5a under autoimmune conditions. Herein, we introduced a new potential strategy for MS treatment and identified an example molecule that acts differentially on Ahr and Arid5a, namely, Flavipin. Furthermore, we provided evidence on the differential actions of Flavipin on Ahr and Arid5a in EAE attenuation and identified *Il23a* as a new mRNA target for Arid5a.

The Ahr PAS-B domain plays crucial roles in the activation of Ahr through interactions with structurally diverse ligands (Fukunaga et al., 1995; Soshilov and Denison, 2008; Corrada et al., 2016). Ligation of Ahr transforms it into a transcriptionally active form that induces transcription of downstream genes such as *Cyp1A1* (Fukasawa et al., 2015) and miR-212/132 cluster (Hanieh and Alzahrani, 2013). The current in silico docking simulation predicted a relatively strong interaction between Flavipin and the mouse Ahr PAS-B domain that comprises five hydrogen bonds and van der Waals forces. This prediction was validated by *in vitro* studies showing that Flavipin induces the gene expression of *Cyp1A1*, miR-132 and miR-212 in $CD4^+$ T cells cultured under Th17 cell-conditions and LPS-stimulated macrophages in an Ahr-dependent manner. The prediction was further supported by comparable results from *in vivo* studies. Furthermore, Flavipin has been reported as an Ahr agonist in human cancer cells (Hanieh et al., 2016).

Computational predictions revealed a potential interaction between Flavipin and Arid5a that comprises three hydrogen bonds and van der Waals forces. It has been demonstrated that Arid5a stabilizes the mRNAs of *Il6*, *Stat3* and *OX40* through physical interaction with their 3′UTR and counteracts the RNase function of Regnase-1 (Masuda et al., 2013; Masuda et al., 2016; Hanieh et al., 2018). Consistently, our results showed that Flavipin abolished the stabilizing effects of Arid5a on the 3′UTR of target mRNAs and reinstated the destabilizing function of Regnase-1. Based on these observations, we conclude that Flavipin inhibits the stabilizing functions of Arid5a and eliminates its competition with Regnase-1 on the 3′UTR of target mRNAs.

Several studies have demonstrated the antioxidant, antimicrobial and anticancer properties of Flavipin (Xiao et al., 2013; Ye et al., 2013; Hanieh et al., 2016). However, to our knowledge, its effects on inflammation and autoimmunity have never been investigated. In the current study, we found that Flavipin exerts anti-inflammatory effects in EAE. These properties of Flavipin were manifested by enhanced generation of $CD4^+FoxP3^+$ T cells, reduced $CD4^+IL\text{-}17^+$ T cells, suppressed IL-6 and TNF-α expression and induction of the miR-132/AChE module. Consistent with these findings, activation of Ahr by exogenous ligands promotes the generation of Treg ($CD4^+FoxP3^+$) cells and reduces that of Th17 ($CD4^+IL\text{-}17^+$) cells in autoimmune models, including EAE (Kaye et al., 2016; Tong et al., 2016; Oh-oka et al., 2017). Moreover, TCDD-activated Ahr suppresses IL-6 and TNF-α, and initiates the anti-inflammatory system by inducing the expression of AChE-targeting miR-132 (Hanieh and Alzahrani, 2013).

It has been demonstrated that Arid5a deficiency alleviates EAE, with suppressed levels of IL-6 and TNF-α and a reduced frequency of $CD4^+IL\text{-}17^+$ T cells, whereas the frequency of $CD4^+FoxP3^+$ T cells was not affected (Masuda et al., 2013). Furthermore, the attenuated EAE in Arid5a-deficient mice manifests as reduced frequencies of $CD4^+IL\text{-}17^+$ and $CD4^+OX40^+$ T cells and fewer $CD4^+CD45^+$ T cells infiltrating within the CNS (Hanieh et al., 2018). In line with these results, Flavipin suppressed IL-6 and TNF-α, reduced the frequencies of $CD4^+IL\text{-}17^+$ and $CD4^+OX40^+$ T cells, and decreased the number of infiltrated $CD4^+CD45^+$ T cells within the CNS. Importantly, Flavipin enhanced the frequency of $CD4^+FoxP3^+$ T cells, a distinguishing feature of EAE attenuation with Ahr activation, indicating that the enhancing effect of Flavipin on $CD4^+FoxP3^+$ T cells was most likely attributed to the activation of Ahr. Taken together, these results indicate that Flavipin attenuates EAE severity through Ahr-dependent and Arid5a-dependent modes of action.

Supporting this conclusion, knockdown of Ahr and Arid5a in $CD4^+$ T cells cultured under Th17- or Treg-inducing conditions and LPS-stimulated macrophages revealed that the suppressive effects of Flavipin on IL-17 and IL-6 were Ahr- and Arid5a-dependent, whereas its enhancing effect on TGF-β and suppressive effect on TNF-α were Ahr-dependent. Furthermore, knockdown of Ahr and Arid5a in $CD4^+$ T cells cultured under Th17-inducing conditions revealed that the suppressive effects of Flavipin on *Stat3* and *OX40* mRNAs were Arid5a-dependent but not Ahr-dependent. The observations and conclusions are consistent with previous reports. For instance, ligand-activated Ahr enhances TGF-β production and suppresses the production of proinflammatory cytokines such as IL-17 and TNF-α (Hanieh and Alzahrani, 2013; Tong et al., 2016; Oh-oka et al., 2017). Moreover, Arid5a targets *Il6* mRNA, increasing its stability, but not *Tnfa* mRNA, and

Arid5a deficiency does not affect TGF-β-producing Treg cells (Masuda et al., 2016). Collectively, the results indicate that Flavipin exerts its anti-inflammatory effects through differential actions on both Ahr and Arid5a.

It has been demonstrated that the production of IL-23, a cytokine required to sustain Th17 cells, is affected by Ahr (Memari et al., 2015; Zhu et al., 2018). However, no studies have shown a relationship between IL-23 and Arid5a. Our results showed that depletion of Arid5a using RNA interference reduces the production of IL-23a. This prompted us to hypothesize that *Il23a* mRNA may be a target for Arid5a. This hypothesis was validated using the luciferase activity of a pGL3 plasmid driven by the *Il23a* 3′UTR, RIP and mRNA stability assays. Together, these findings introduce *Il23a* as a new mRNA target for Arid5a and provide evidence related to the pro-inflammatory roles of Arid5a.

In summary, we found that Flavipin attenuates EAE *via* Ahr-dependent and Arid5a-dependent mechanisms. It activates Ahr to promote the differentiation of Treg cells and suppress proinflammatory mediators and inhibits the stabilizing functions of Arid5a on target mRNAs encoding related mediators. We also identified *Il23a* as a new target mRNA for Arid5a. The current study reveals a new therapeutic strategy for autoimmune conditions, such as MS, in which the functions of Ahr and Arid5a are differentially manipulated.

CRediT authorship contribution statement

Abdullah Alzahrani: Funding acquisition, Conceptualization, Investigation, Methodology, Data curation, Writing - review & editing. **Hamza Hanieh:** Conceptualization, Investigation, Methodology, Formal analysis, Project administration, Writing - review & editing.

Declaration of Competing Interest

The authors declare that they have no known competing financial interests or personal relationships that could have appeared to influence the work reported in this paper.

Acknowledgment

We thank Professor Tadamitsu Kishimoto, Osaka University, Japan, for providing plasmids, and Doctor Mahdi Farhan, International Medical Research Center (IMReC), Jordan/UniTechPharma, Switzerland, for technical, medical and pharmaceutical guidance. This work was supported by the Deanship of Scientific Research, King Faisal University, Saudi Arabia [Annual Research Project Track, grant number 170099].

Appendix A. Supplementary material

Supplementary data to this article can be found online at https://doi.org/10.1016/j.jsps.2020.10.007.

References

Alzahrani, A., Maged, M., Hairul-Islam, M.I., Osama, A., Maha, M., Alfuwaires, M., Hanieh, H., 2019. Activation of aryl hydrocarbon receptor signaling by a novel agonist ameliorates autoimmune encephalomyelitis. PLoS One 14, e0215981.

Alzahrani, A., Hanieh, H., Hairul-islam, M.I., Mohafez, O., Shehata, T., Bani Ismail, M., Alfwuaires, M., 2017. Enhancing miR-132 expression by aryl hydrocarbon receptor attenuates tumorigenesis associated with chronic colitis. Int. Immunopharmacol. 52, 342–351.

Amatya, N., Childs, E.E., Cruz, J.A., Aggor, F.E.Y., Garg, A.V., Berman, A.J., et al., 2018. IL-17 integrates multiple self-reinforcing, feed-forward mechanisms through the RNA binding protein Arid5a. Sci. Signaling 11 (551), eaat4617.

Chinen, C., Nakahama, T., Kimura, A., Nguyen, N.T., Takemori, H., Kumagai, A., et al., 2015. The aryl hydrocarbon receptor/microRNA-212/132 axis in T cells regulates IL-10 production to maintain intestinal homeostasis. Int. Immunol. 27 (8), 405–415.

Corrada, D., Soshilov, A.A., Denison, M.S., Bonati, L., 2016. Deciphering dimerization modes of PAS domains: Computational and experimental analyses of the AhR: ARNT complex reveal new insights into the mechanisms of AhR transformation. PLoS Comput. Biol. 12, (6) e1004981.

Douglas, J.N., Gardner, L.A., Salapa, H.E., Lalor, S.J., Lee, S., Segal, B.M., et al., 2016. Antibodies to the RNA-binding protein hnRNP A1 contribute to neurodegeneration in a model of central nervous system autoimmune inflammatory disease. J. Neuroinflammat. 13 (1), 178.

Fukasawa, K., Kagaya, S., Maruyama, S., Kuroiwa, S., Masuda, K., Kameyama, Y., et al., 2015. A novel compound, NK150460, exhibits selective antitumor activity against breast cancer cell lines through activation of aryl hydrocarbon receptor. Mol. Cancer Ther. 14 (2), 343–354.

Fukunaga, B.N., Probst, M.R., Reisz-Porszasz, S., Hankinson, O., 1995. Identification of functional domains of the aryl hydrocarbon receptor. J. Biol. Chem. 270 (49), 29270–29278.

Garg, A.V., Amatya, N., Chen, K., Cruz, J.A., Grover, P., Whibley, N., et al., 2015. MCPIP1 endoribonuclease activity negatively regulates interleukin-17-mediated signaling and inflammation. Immunity 43 (3), 475–487.

Hanieh, H., 2015. Aryl hydrocarbon receptor-microRNA-212/132 axis in human breast cancer suppresses metastasis by targeting SOX4. Mol. Cancer 14, 172.

Hanieh, H., Alzahrani, A., 2013. MicroRNA-132 suppresses autoimmune encephalomyelitis by inducing cholinergic anti-inflammation: A new Ahr-based exploration. Eur. J. Immunol. 43 (10), 2771–2782.

Hanieh, H., 2014. Toward understanding the role of aryl hydrocarbon receptor in the immune system: current progress and future trends. Biomed. Res. Int. 2014, 520763.

Hanieh, H., Masuda, K., Metwally, H., Chalise, J.P., Mohamed, M., Nyati, K.K., et al., 2018. Arid5a stabilizes OX40 mRNA in murine CD4$^+$ T cells by recognizing a stem-loop structure in its 3′ UTR. Eur. J. Immunol. 48 (4), 593–604.

Hanieh, H., Mohafez, O., Hairul-Islam, V.I., Alzahrani, A., Bani Ismail, M., Thirugnanasambantham, K., 2016. Novel aryl hydrocarbon receptor agonist suppresses migration and invasion of breast cancer cells. PLoS One 11 (12), e0167650.

Kaye, J., Piryatinsky, V., Birnberg, T., Hingaly, T., Raymond, E., Kashi, R., 2016. Laquinimod arrests experimental autoimmune encephalomyelitis by activating the aryl hydrocarbon receptor. Proc. Nat. Acad. Sci. USA 113 (41), E6145–E6152.

Lis, M., Kim, T., Sarmiento, J.J., Kuroda, D., Dinh, H.V., Kinjo, A.R., et al., 2011. Bridging the gap between single-template and fragment based protein structure modeling using Spanner. Immunome Res. 7 (1), 1–8.

Masuda, K., Kimura, A., Hanieh, H., Nguyen, N.T., Nakahama, T., Chinen, I., et al., 2011. Aryl hydrocarbon receptor negatively regulates LPS-induced IL-6 production through suppression of histamine production in macrophages. Int. Immunol. 23 (10), 637–645.

Masuda, K., Kishimoto, T., 2018. A potential therapeutic target RNA-binding protein, Arid5a for the treatment of inflammatory disease associated with aberrant cytokine expression. Curr. Pharm. Des. 24 (16), 1766–1771.

Masuda, K., Ripley, B., Nishimura, R., Mino, T., Takeuchi, O., Shioi, G., 2013. Arid5a controls IL-6 mRNA stability, which contributes to elevation of IL-6 level in vivo. Proc. Nat. Acad. Sci. USA 110 (23), 9409–9414.

Masuda, K., Ripley, B., Nyati, K.K., Dubey, P.K., Zaman, M.M., Hanieh, H., et al., 2016. Arid5a regulates naive CD4$^+$ T cell fate through selective stabilization of Stat3 mRNA. J. Exp. Med. 213 (4), 605–619.

Memari, B., Bouttier, M., Dimitrov, V., Ouellette, M., Behr, M.A., Fritz, J.H., White, J.H., 2015. Engagement of the aryl hydrocarbon receptor in mycobacterium tuberculosis–infected macrophages has pleiotropic effects on innate immune signaling. J. Immunol. 195 (9), 4479–4491.

Metwally, H., Tanaka, T., Li, S., Parajuli, G., Kang, S., Hanieh, H., et al., 2020. Noncanonical STAT1 phosphorylation expands its transcriptional activity into promoting LPS-induced IL-6 and IL-12p40 production. Sci. Signaling 13 (624), eaay0574.

Nakahama, T., Hanieh, H., Nguyen, N.T., Chinen, I., Ripley, B., Millrine, D., et al., 2013. Aryl hydrocarbon receptor-mediated induction of the microRNA-132/212 cluster promotes interleukin-17–producing T-helper cell differentiation. Proc. National Acad. Sci. USA 10 (29), 11964–11969.

Nakahama, T., Kimura, A., Nguyen, N.T., Chinen, I., Hanieh, H., Nohara, K., et al., 2011. Aryl hydrocarbon receptor deficiency in T cells suppresses the development of collagen-induced arthritis. Proc. Nat. Acad. Sci. USA 108 (34), 14222–14227.

Nguyen, N.T., Hanieh, H., Nakahama, T., Kishimoto, T., 2013. The roles of aryl hydrocarbon receptor in immune responses. Int. Immunol. 25 (6), 335–343.

Nyati, K.K., Agarwal, R.G., Sharma, P., Kishimoto, T., 2019. Arid5a regulation and the roles of Arid5a in the inflammatory response and disease. Front. Immunol. 10, 2790.

Oh-Oka, K., Kojima, Y., Uchida, K., Yoda, K., Ishimaru, K., Nakajima, S., 2017. Induction of colonic regulatory T cells by mesalamine by activating the aryl hydrocarbon receptor. Cell. Mol. Gastroenterol. Hepatol. 4 (1), 135–151.

Patial, S., Curtis 2nd, A.D., Lai, W.S., Stumpo, D.J., Hill, G.D., Flake, G.P., Mannie, M.D., Blackshear, P.J., 2016. Enhanced stability of tristetraprolin mRNA protects mice against immune-mediated inflammatory pathologies. Proc. Nat. Acad. Sci. USA 113 (7), 1865–1870.

Rothhammer, V., Mascanfroni, I.D., Bunse, L., Takenaka, M.C., Kenison, J.E., Mayo, L., et al., 2016. Type I interferons and microbial metabolites of tryptophan modulate astrocyte activity and central nervous system inflammation via the aryl hydrocarbon receptor. Nat. Med. 22 (6), 586–597.

Sadri, N., Schneider, R.J., 2009. Auf1/Hnrnpd-deficient mice develop pruritic inflammatory skin disease. J. Invest. Dermatol. 129 (3), 657–670.

Salapa, H.E., Libner, C.D., Levin, M.C., 2020. Dysfunctional RNA-binding protein biology and neurodegeneration in experimental autoimmune encephalomyelitis in female mice. J. Neurosci. Res. 98 (4), 704–717.
Söding, J., Biegert, A., Lupas, A.N., 2005. The HHpred interactive server for protein homology detection and structure prediction. Nucleic Acids Res. 33, W244–W248.
Soshilov, A., Denison, M.S., 2008. Role of the Per/Arnt/Sim domains in ligand-dependent transformation of the aryl hydrocarbon receptor. J. Biol. Chem. 283 (47), 32995–33005.
Srinivasan, S., Severa, M., Rizzo, F., Menon, R., Brini, E., Mechelli, R., et al., 2017. Transcriptional dysregulation of Interferome in experimental and human Multiple Sclerosis. Sci. Rep. 7 (1), 8981.
Tong, B., Yuan, X., Dou, Y., Wu, X., Chou, G., Wang, Z., et al., 2016. Norisoboldine, an isoquinoline alkaloid, acts as an aryl hydrocarbon receptor ligand to induce intestinal Treg cells and thereby attenuate arthritis. Int. J. Biochem. Cell Biol. 75, 63–73.
Van Schependom, J., Guldolf, K., D'hooghe, M.B., Nagels, G., D'haeseleer, M., 2019. Detecting neurodegenerative pathology in multiple sclerosis before irreversible brain tissue loss sets in. Translational Neurodegenerat. 8, 37.
Xiao, Y., Li, H.X., Li, C., Wang, J.X., Li, J., Wang, M.H., Ye, Y.H., 2013. Antifungal screening of endophytic fungi from Ginkgo biloba for discovery of potent anti-phytopathogenic fungicides. FEMS Microbiol. Lett. 339 (2), 130–136.
Yan, Z., Gibson, S.A., Buckley, J.A., Qin, H., Benveniste, E.N., 2018. Role of the JAK/STAT signaling pathway in regulation of innate immunity in neuroinflammatory diseases. Clin. Immunol. 189, 4–13.
Ye, Y., Xiao, Y., Ma, L., Li, H., Xie, Z., Wang, M., 2013. Flavipin in Chaetomium globosum CDW7, an endophytic fungus from Ginkgo biloba, contributes to antioxidant activity. Appl. Microbiol. Biotechnol. 97 (16), 7131–7139.
Yoshinaga, M., Takeuchi, O., 2019. RNA binding proteins in the control of autoimmune diseases. Immunol. Med. 42 (2), 53–64.
Zaman, M.M., Masuda, K., Nyati, K.K., Dubey, P.K., Ripley, B., Wang, K., et al., 2016. Arid5a exacerbates IFN-γ–mediated septic shock by stabilizing T-bet mRNA. Proc. Nat. Acad. Sci. USA 113 (41), 11543–11548.
Zhu, J., Luo, L., Tian, L., Yin, S., Ma, X., Cheng, S., et al., 2018. Aryl hydrocarbon receptor promotes IL-10 expression in inflammatory macrophages through Src-STAT3 signaling pathway. Front. Immunol. 9, 2033.